

## Corrosion Inhibition of Carbon Steel in H<sub>2</sub>SO<sub>4</sub> By *Chenopodium Ambrosioides*

E. Rodriguez-Clemente<sup>1</sup>, J.G. Gonzalez-Rodriguez<sup>1,\*</sup>, G. Valladarez<sup>2</sup>, G.F. Dominguez-Patiño<sup>2</sup>

<sup>1</sup> Universidad Autonoma del Estado de Morelos, CIICAP, Av. Universidad 1001, 62209-Cuernavaca, Mor., Mexico

<sup>2</sup> Universidad Autonoma del Estado de Morelos, Facultad de Ciencias Quimicas e Ing., Av. Universidad 1001, 62209-Cuernavaca, Mor., Mexico

\*E-mail: [ggonzalez@uaem.mx](mailto:ggonzalez@uaem.mx)

Received: 6 October 2011 / Accepted: 9 November 2011 / Published: 1 December 2011

---

*Chenopodium ambrosioides* leaves extract has been investigated as a carbon steel corrosion inhibitor in 0.5 M sulfuric acid by using electrochemical techniques and weight loss tests at different concentrations and temperatures. Results have shown that inhibition efficiency reaches its highest value at 25 ppm, decreasing with either lower or higher inhibitor concentrations. Inhibitor efficiency increases with temperature, decreases with the acid concentration and reaches a maximum value after 12 hours of exposure and it decreases for longer exposure times. It was found that the inhibitory effect is due to the presence of nitrates on this extract.

---

**Keywords:** Carbon steel, corrosion, *Chenopodium ambrosioides*

### 1. INTRODUCTION

Due to the currently imposed requirements for eco-friendly corrosion inhibitors, there is a growing interest in the use of natural products such as leaves or seeds extracts. Some papers have reported the use of natural products for mild steel corrosion inhibition in different environments [1-21]. This is due to the fact that synthetic inhibitors are expensive, highly toxic for human beings and other living species, among other factors. Among the so-called "green inhibitors" are organic compounds that act by adsorption on the metal surface such as ascorbic acid, succinic acid, tryptamine, caffeine. Additionally, some other natural products such as black pepper, *Azadirachta indica*, *Gossipium hirsutum*, guanadine, *Occimum viridis*, *Talferia occidentalis* and *Hibiscus sabdariffa*, have been used. The corrosion efficiency of these extracts is normally ascribed to the presence, in their composition, of

complex organic species such as tannins, alkaloids and nitrogen bases, carbohydrates and proteins as well as their acid hydrolysis products.

Despite the great availability and variety of plant materials, only relatively few have been thoroughly investigated. The present report continues to focus on the broadening application of plant extracts for metallic corrosion control with some plant leaves extracts of *Chenopodium ambrosioides* for carbon steel in acidic solutions. *Chenopodium ambrosioides* is a plant widely used in caribbean and latinoamerican not only in the cuicin but also as ethnic medicin from ancient times because it conatains up to 70% ascaridol with products of a monoterpenic (C10) and sesquiterpenic (C15) nature. Additionally, it has been found the presence of limonene, transpine carveol, aritasone,  $\beta$ -pinene, mircene, felandrene, alcanfor and terpeneol

Iron and steels are the most widely used materials exposed to the atmosphere and acidic environments in industrial applications due to their low cost and avaiability [21]. Aqueous solutions of hydrochloric and sulfuric acid are extensively used in acid cleaning, pickling and descaling processes as well as for drilling operations [22, 23]. Corrosion rates of both materials when exposed to acidic solutions are high, and therefore, it is necessary the use of novel corrosion control methods environmentally friendly. Thus, the aim of this work, is to gain some insight in the corrosion resistance of carbon steel in sulfuric acid in presence of a widely available plant such as *Chenopodium ambrosioides* by using both gravimetric and electrochemical techniques.

## 2. EXPERIMENTAL PROCEDURE

Corrosion tests were performed on coupons prepared from 1018 carbon steel rods containg 0.14%C, 0.90% Mn, 0.30%S, 0.030% P and as balance Fe, encapsulated in commercial epoxic resin with an exposed area of 1.0 cm<sup>2</sup>. The aggressive solution, 0.5 M H<sub>2</sub>SO<sub>4</sub> was prepared by dilution of analytical grade H<sub>2</sub>SO<sub>4</sub> with double distilled water. Dried *C. ambrosioides* leaves were soaked in hexane during 24 h and refluxed during 5 h obtaining a solid, wich was weighted and dissolved in methanol and used as a stock solution and used then for preparation of the desired concentrations by dilution, i.e. 0, 5, 10, 25, 50 and 100 ppm. Weight loss experiments were carried out with steel rods 2.5 cm length and 0.6 cm diameter abraded with fine emery paper until 1200 grade, rinsed with acetone, and exposed to the aggressive solution during 72 h. After a total time of exposition of 72 hours, specimens were taken out, washed with distilled water, degreased with acetone, dried and weighed accurately. Tests were performed by triplicate at room temperature (25 °C), 40 and 60 °C by using a hot plate. Corrosion rates, in terms of weight loss measurements,  $\Delta W$ , were calculated as follows:

$$\Delta W = (m_1 - m_2) / A \quad [1]$$

were  $m_1$  is the mass of the specimen before corrosion,  $m_2$  the mass of the specimen after corrosion, and  $A$  the exposed area of the specimen. For the weight loss tests, inhibitor efficiency,  $IE$ , was calculated as follows:

$$IE (\%) = 100 (\Delta W_1 - \Delta W_2) / \Delta W_1 \quad [2]$$

were  $\Delta W_1$  is the weight loss without inhibitor, and  $\Delta W_2$  the weight loss with inhibitor. Specimens were removed, rinsed in water and in acetone, dried in warm air and stored in a desiccator. Specimens were weighed in an analytical balance with a precision of 0.1 mg. Electrochemical techniques employed included potentiodynamic polarization curves and electrochemical impedance spectroscopy measurements, EIS. In all experiments, the carbon steel electrode was allowed to reach a stable open circuit potential value,  $E_{\text{corr}}$ . Polarization curves were recorded at a constant sweep rate of 1 mV/s at the interval from -500 to +500 mV respect to the  $E_{\text{corr}}$  value. Measurements were obtained by using a conventional three electrodes glass cell with two graphite electrodes symmetrically distributed and a saturated calomel electrode (SCE) as reference with a Lugging capillary bridge. Corrosion current density values,  $i_{\text{corr}}$ , were obtained by using Tafel extrapolation. Electrochemical impedance spectroscopy tests were carried out at  $E_{\text{corr}}$  by using a signal with amplitude of 10 mV in a frequency interval of 100 mHz-100 KHz. An ACM potentiostat controlled by a desk top computer was used for the polarization curves, whereas for the EIS measurements, a model PC4 300 Gamry potentiostat was used.

### 3. RESULTS AND DISCUSSION

**Table 1.** Effect of *C. ambrosioides* concentration and temperature on the weight loss and inhibitor efficiency.

$C_{\text{inh}}$ (ppm)	25 °C		40 °C		60 °C	
	Mass loss (mg/ cm <sup>2</sup> )	IE (%)	Mass loss (mg/ cm <sup>2</sup> )	IE (%)	Mass loss (mg/ cm <sup>2</sup> )	IE (%)
0	268	----	2035	-----	2335	-----
5	215	-2.5	1365	33	701	70
10	220	20	936	53	1167.5	50
25	133.5	50	467	70	610	80
50	131	49	514	44	1140	78
100	215	-2.5	653	63	731	73

Table 1 shows the effect of *C. ambrosioides* concentration and temperature on the weight loss results and inhibitor efficiency for 1018 carbon steel in 0.5 M H<sub>2</sub>SO<sub>4</sub> whereas Fig. 1 shows the effect of inhibitor concentration on the inhibitor efficiency at the different tested temperatures. It can be seen that as the inhibitor concentration increases, the inhibitor efficiency increases reaching a maximum value at 25 ppm, decreasing with a further increase in the inhibitor concentration. It can also be seen that by increasing the testing temperature, the corrosion rate increases but the inhibitor efficiency increases too, which suggests that the corrosion inhibition might be caused by the inhibitor adsorption onto the steel surface from the acidic solution, and higher temperatures might cause a stronger adsorption of the inhibitor on the steel surface.

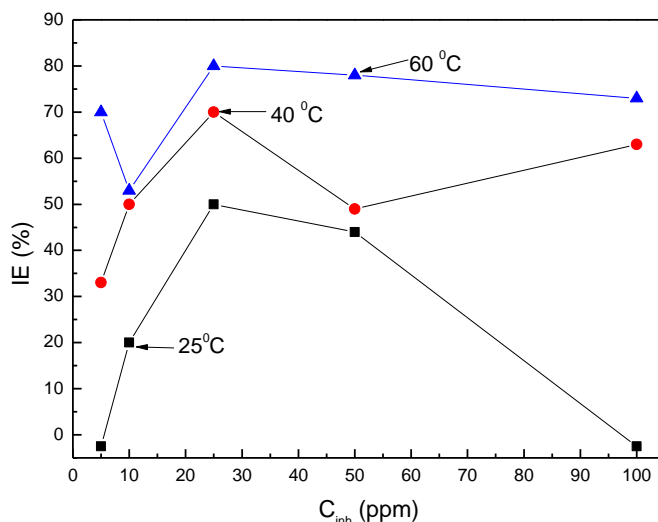


**Figure 1.** Effect of *C. ambrosioides* concentration on the inhibitor efficiency for 1018 carbon steel in 0.5 M H<sub>2</sub>SO<sub>4</sub> at different testing temperatures.

The apparent activation energy,  $E_a$ , associated with 1018 carbon steel in uninhibited and inhibited acid solution was determined by using an Arrhenius-type plot according to the following equation:

$$\log \Delta W = -E_a / 2.303RT + \log F \quad [3]$$

where  $\Delta W$  is defined in eq. [2],  $R$  is the molar gas constant,  $T$  is the absolute temperature and  $F$  is the frequency factor.

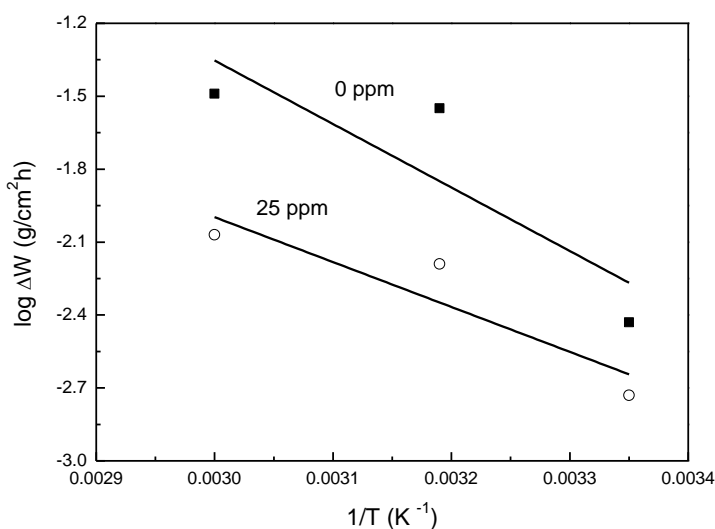


**Figure 2.** Arrhenius plot for 1018 carbon steel in 0.5 M H<sub>2</sub>SO<sub>4</sub> solution containing 0 and 25 ppm of *C. ambrosioides*.

Arrhenius plots of (log ΔW) against 1/T for 1018 carbon steel in 0.5 M H<sub>2</sub>SO<sub>4</sub> in absence and presence of *C. ambrosioides* is shown in Fig. 2. The apparent activation energy obtained for the corrosion process in the free acid solution was found to be 26.1 and 18.46 kJ mol<sup>-1</sup> in the presence of the inhibitor. Notably, the energy barrier of the corrosion reaction decreased in the presence of the inhibitor, which can be due to the chemisorption of the inhibitor on the steel surface.

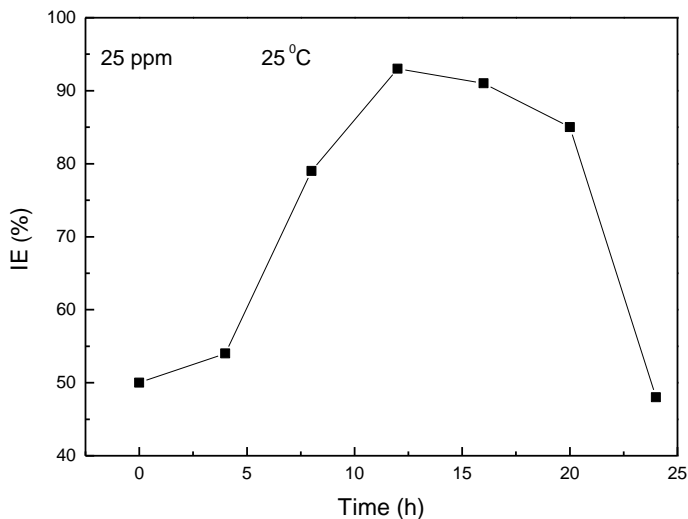


**Figure 3.** Variation of inhibitor efficiency with time for 1018 carbon steel in 0.5 M H<sub>2</sub>SO<sub>4</sub> containing 25 ppm *C. ambrosioides*.

In order to have an insight on the stability of any inhibitor-formed film on the steel surface at 25 ppm and 25 °C, a variation of the inhibitor efficiency with time was plotted versus time, showing the results in Fig. 3.

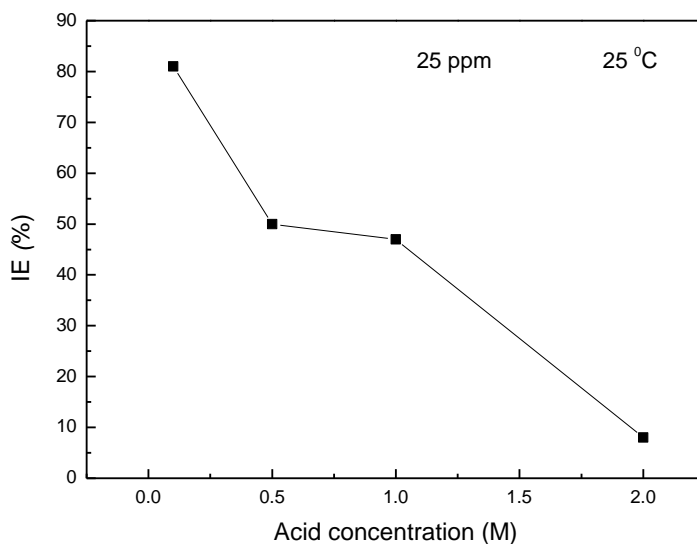


**Figure 4.** Effect of the sulfuric acid concentration on the *C. ambrosioides* efficiency for 1018 carbon steel.

This figure shows that the inhibitor efficiency increases as time elapses, reaching a maximum value around 12 hours, decreasing with a further increase in the testing time, indicating a desorption process of the inhibitor for long exposure times and a deterioration of the protective inhibitor formed film on the metal surface. Finally, Fig. 4 shows the effect of the acid concentration on the inhibitor efficiency at 25 ppm and 25 °C, where it can be seen that as the acid concentration increases, the inhibitor efficiency decreases from 80%, the inhibitor efficiency obtained with 0.1 M H<sub>2</sub>SO<sub>4</sub>, down to an inhibitor efficiency value of 10% obtained with 2.0 M H<sub>2</sub>SO<sub>4</sub>. Similar results were obtained by Quraishi et al. [5,24] with *Murraya koenigii* leaves and by *Black pepper* extract. However, they evaluated carbon steel in both HCl and H<sub>2</sub>SO<sub>4</sub> by using *Murraya koenigii* and obtained higher efficiency values with H<sub>2</sub>SO<sub>4</sub>, between 96-98%, than that in HCl, which fluctuated between 88-92%. Similarly, In the former, the efficiency increased as time elapsed whereas in the later increased by increasing the acid concentration but it decreased with a further increase in the acid concentration. Nevertheless, in most cases, the inhibitor efficiency increases with increasing the inhibitor concentration, as shown by Oguzie [20] who evaluated the inhibition efficiency of carbon steel in H<sub>2</sub>SO<sub>4</sub> by *Occimum viridis*, *Azadirachta indica*, *Hibiscus sabdariffa*, *Telferia occidentalis* and *Garcinia kola*.

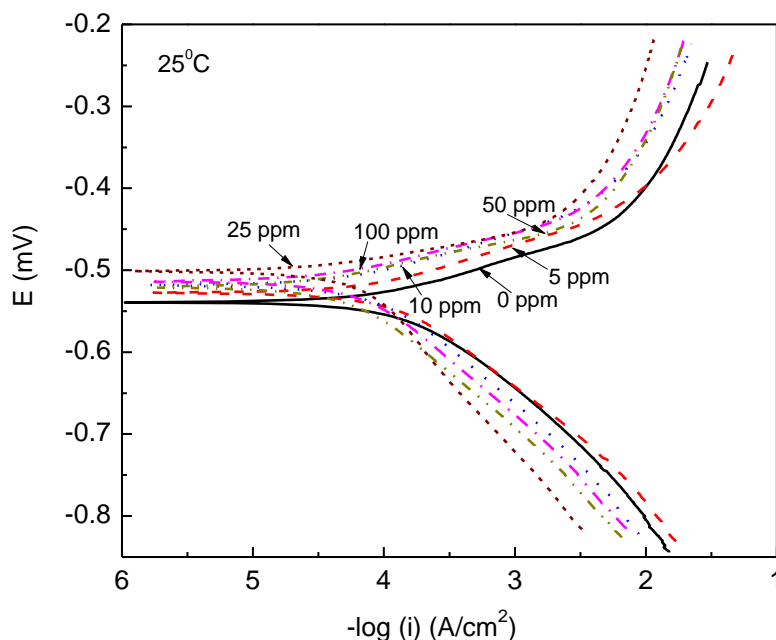


**Figure 5.** Effect of *C. ambrosioides* concentration in the polarization curves for 1018 carbon steel in 0.5 M H<sub>2</sub>SO<sub>4</sub> at different testing temperatures.

Two main types of interaction often describe adsorption of organic inhibitors on a corroding metal surface: chemical adsorption and physical adsorption [25-28]. It has been suggested that physisorbed molecules are attached to the metal at local cathodes and essentially retard metal dissolution by stifling the cathodic reaction whereas chemisorbed molecules protect anodic areas and reduce the inherent reactivity of the metal at the sites where they are attached. The more efficient inhibitors appear to protect anodic areas preferentially by chemisorption. [24, 26, 29]. Analysis of the

temperature dependence of inhibition efficiency gives some insight into the possible mechanism of inhibitor adsorption [27]. A decrease in inhibition efficiency with rise in temperature is frequently interpreted as being suggestive of formation of an adsorption film by physical, electrostatic, nature. The reverse effect, corresponding to a an increase in inhibition efficiency with rise in temperature suggests a chemisorption mechanism [28, 29]. From the foregoing, the trend for *C. ambrosioides* suggests physisorption of inhibiting species.

**Table 2.** Electrochemical parameters obtained from polarization curves at 25 °C.

$C_{inh}$ (ppm)	$E_{corr}$ (mV)	$i_{corr}$ (A/cm <sup>2</sup> )	$\beta_a$ (mV/dec)	$\beta_c$ (mV/dec)
0	-538	$1 \times 10^{-4}$	46	104
5	-525	$9.7 \times 10^{-5}$	43	112
10	-514	$5.7 \times 10^{-5}$	40	125
25	-501	$3.1 \times 10^{-5}$	29	176
50	-522	$3.3 \times 10^{-5}$	35	137
100	-517	$5.3 \times 10^{-5}$	43	130

The effect of *C. ambrosioides* concentration in the polarization curves at 25 °C is shown on Fig. 5 whereas electrochemical parameters for these curves are shown in table 2. It can be seen that there is no evidence of a passive film formation neither without inhibitor nor with it; the addition of *C. ambrosioides* has caused a clear decreases in both the anodic and cathodic branch of the polarization curves, and this effect is more pronounced as the inhibitor concentration increases; as soon as the extract is added to the electrolyte, the  $E_{corr}$  value becomes nobler, reaching its highest value when 25 ppm of inhibitor is added, decreasing its value with a further increase in the inhibitor concentration. Additionally, the  $i_{corr}$  value decreases as the inhibitor concentration increases, reaching its lowest value with the addition of 25 ppm, increasing once again with a further increase in the inhibitor dosis. Quraishi et al. [24] with *Black pepper* extract obtained  $i_{corr}$  values of 8.5, 4.5 and  $3.4 \times 10^{-5}$  A/cm<sup>2</sup> by adding 30, 60 and 100 ppm of extract respectively, very similar results values to the ones found in this work. On the other hand when he used *Murraya koenigii* leaves, the  $i_{corr}$  values obtained were  $17.6 \times 10^{-5}$  A/cm<sup>2</sup> when added 180 ppm of extract. Tis value decreased to 7.1, 4.8 and  $4.1 \times 10^{-5}$  A/cm<sup>2</sup> but with the addition of 240, 300 and 600 ppm of extract respectively, i.e. corrosion rates similar to ours but with much higher inhibitor concentrations. The anodic slope was practically unaffected by the addition of the *C. ambrosioides*, which indicates that adsorbed inhibitor does not affect the metal dissolution process; unlike this, the cathodic slope value increases as the inhibitor concentration increases, reaching its highest value with the addition of 25 ppm, decreasing with a further increase in the inhibitor dosis. This means that the *C. ambrosioides* acts as a cathodic type inhibitor, affecting the hydrogen evolution reaction, which is diminished exclusively by the surface-blocking effect

Niquist and Bode diagrams for 1018 carbon steel exposed to 0.5 M H<sub>2</sub>SO<sub>4</sub> with different *C. ambrosioides* dosis is shown in Fig. 6. Niquist diagram, Fig. 6a, show a single depressed, capacitive semicircle with its center in the real axis regardless of the inhibitor concentration, indicating that the corrosion process is under charge transfer from the metal to the electrolyte through the double

electrochemical layer. This type of plot is characteristic of solid electrodes and is often ascribed to dispersion effects, which have been attributed to roughness and inhomogeneities of the surface during corrosion [25, 26]. This behavior is not affected by the presence of the inhibitor, indicating the activation-controlled nature of the reaction; the semicircle diameter increases with the inhibitor concentration, reaching a maximum value with 25 ppm of inhibitor, decreasing with a further increase in the inhibitor dose.

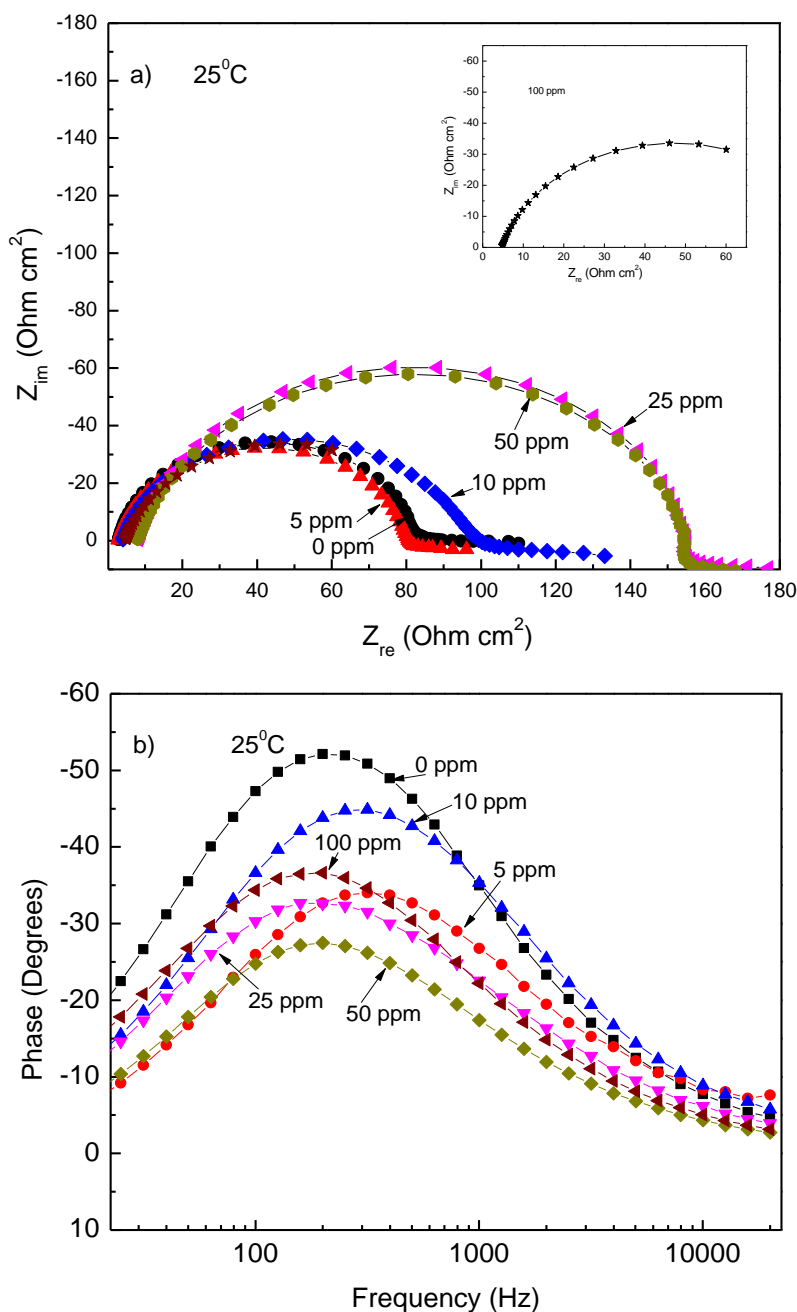


**Figure 6.** Effect of *C. ambrosioides* concentration in the a) Nyquist and b) Bode diagrams for 1018 carbon steel in 0.5 M H<sub>2</sub>SO<sub>4</sub> at different testing temperatures.

The semicircle diameter is related to the charge transfer resistance,  $R_{ct}$ , inversely proportional to the  $i_{corr}$  value, thus, the lowest corrosion rate is attained with 25 ppm, just as indicated by the weight loss results in Fig. 1 and table 1.

Bode diagram, Fig. 6b, shows a single peak around 200 Hz, which shifts towards lower frequency values as the inhibitor concentration increases up to 25 ppm; with a further increase in the inhibitor concentration, this peak returns towards higher frequency values, to the position found in the uninhibited solution.

Quraishi et al. [24] with *Black pepper* extract obtained  $R_{ct}$  values of 350, 500 and 1000 ohm  $cm^2$  by adding 30, 60 and 100 ppm of extract respectively and when he used *Murraya koenigii* leaves [5] these values were between 50 and 180 ohm  $cm^2$ , very similar to the values obtained in the present work.

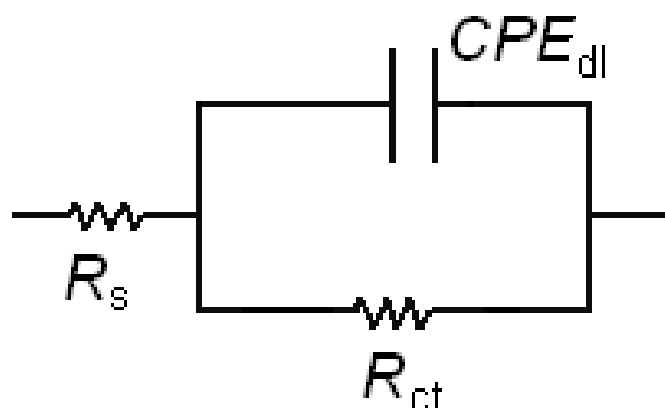


**Figure 7.** Electric circuit used to simulate the EIS data for 1018 carbon steel in 0.5 M  $H_2SO_4$  with different doses of *C. ambrosioides* extract.

Equivalent electric circuit used to simulate the EIS data for 1018 carbon steel exposed to 0.5 M  $H_2SO_4$  with different *C. ambrosioides* dosis is shown in Fig. 7. In this figure,  $R_s$  represents the solution resistance,  $R_{ct}$  the charge transfer resistance,  $CPE_{dl}$  the constant phase element of the double electrochemical layer. The impedance of a CPE is described by the expression:

$$Z_{CPE} = Y^{-1} (j\omega)^{-n} \quad [3]$$

where  $Y$  is the admittance,  $j$  is  $\sqrt{-1}$ ,  $\omega$  is  $2\pi f$  and  $n$  has the meaning of a phase shift. Thus, it can be seen that the  $R_{ct}$  value reaches its highest value between 25 and 50 ppm, whereas the double electrochemical layer admittance value,  $Y_{dl}$ , attains its lowest value at these inhibitor concentrations, which may be attributable to the adsorption of the components in the *C. ambrosioides* extract onto the metal/electrolyte interface or to an increase of the double electrochemical layer [12].

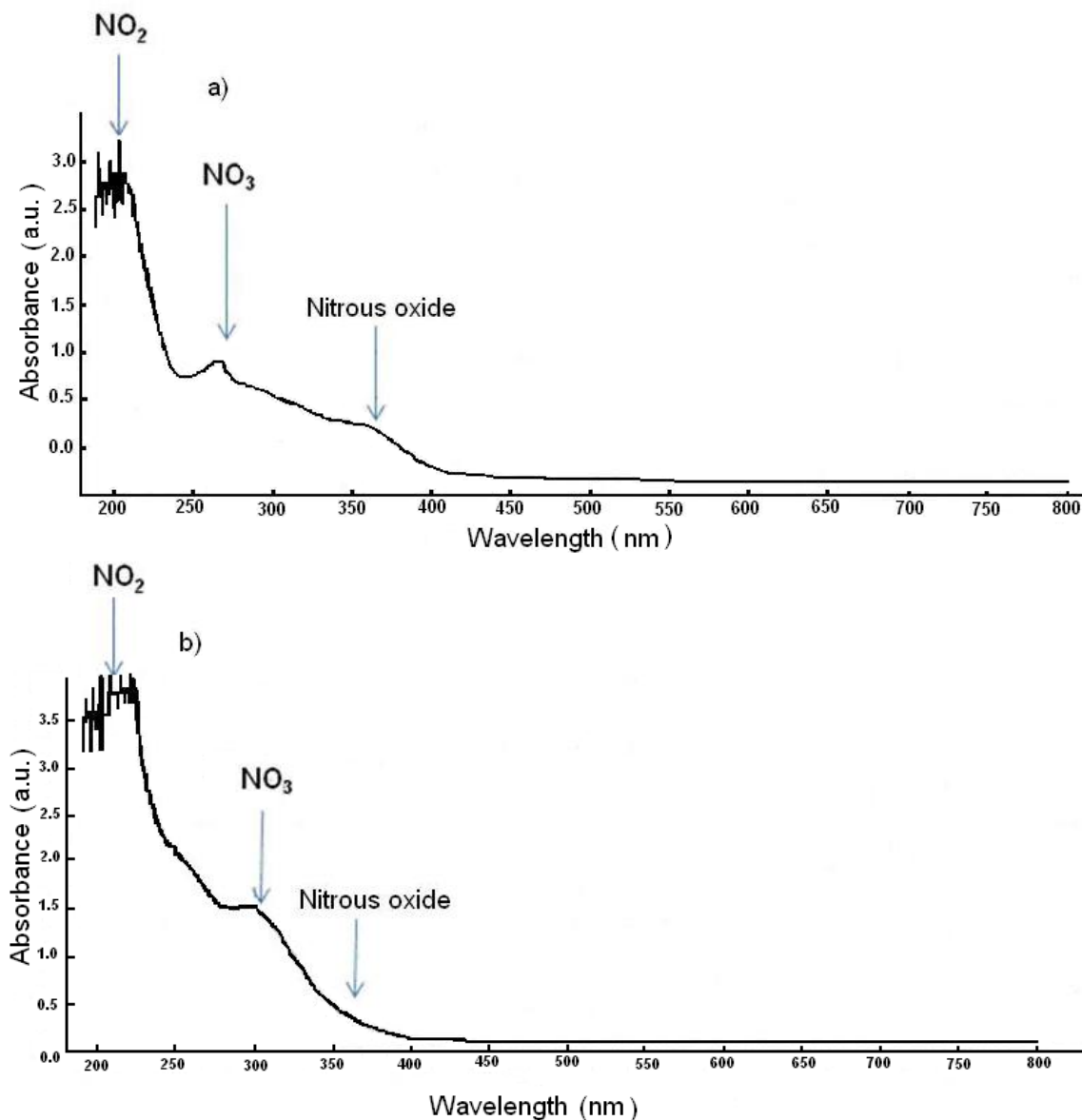


**Figure 8.** UV-spectrum of the *C. ambrosioides* extract a) before and b) after corrosion test.

UV and IR spectra analysis were performed for the acidic solution containing the extract before and after the corrosion test. For the extract before the corrosion test, the UV-spectrum shows an absorption peak between 260-270 nm, Fig. 8, corresponding to nitrates; this Peak shifts towards 325 nm a 350 nm probably due to the formation of nitrites due to the reduction of nitrates. After the corrosion tests, there is now an absorption peak at 302 nm, which can be due to the presence of nitrous oxide, due to the reduction of nitrites. On the other hand, the IR spectrum for the solution before the corrosion test, Fig. 9 a, shows a peak at  $3420\text{ cm}^{-1}$ , due to the stretching of the O-H groups; the peaks observed at  $2926$  and  $2858\text{ cm}^{-1}$  correspond to the C-H links, the one observed at  $1630\text{ cm}^{-1}$  corresponds to the C=O group; the one observed at  $1385\text{ cm}^{-1}$  corresponds to the  $\text{NO}_2$  group whereas the one found at  $1100\text{ cm}^{-1}$  is due to stretching of C-N.

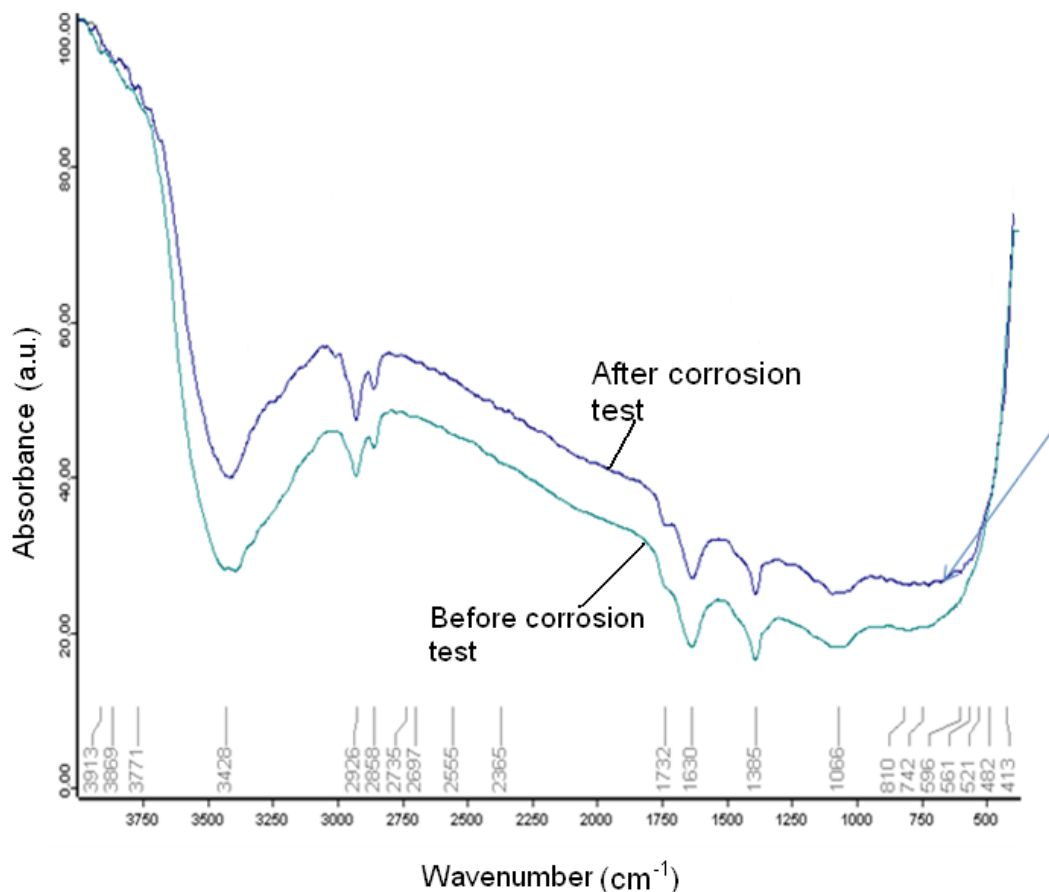


**Figure 9.** IR-spectrum of the *C. ambrosioides* extract before and after corrosion test.

**Table 4.** Frequencies and adsorption peaks of IR for *C. ambrosioides* extract

0.5 M H <sub>2</sub> SO <sub>4</sub> + 25 ppm extract before corrosion test		0.5 M H <sub>2</sub> SO <sub>4</sub> + 25 ppm extract after corrosion test	
Frequency (cm <sup>-1</sup> )	Assignment	Frequency (cm <sup>-1</sup> )	Assignment
3428	O-H stretch	3428	O-H stretch
2926	O-H stretch	2926	-OH stretch
2858	C-H stretch	2858	C-H stretch
1732	C=O stretch		
1630	N-H bending	1630	N-H bending
1385	C-H bending	1385	C-H bending

After the corrosion experiment, Fig. 9 b, there appear absorption bands at 520 and 560 cm<sup>-1</sup> due to the C-H links, another peaks at 825 and 900 cm<sup>-1</sup> due to the formation of C-S-C links, and another one at 1069 cm<sup>-1</sup> due to the C=S links; the intensity of the peak observed at 1385 cm<sup>-1</sup> increases, which corresponds to the NO<sub>2</sub> group; the peak present at 1125 cm<sup>-1</sup> corresponds to the C-N links, whereas the one present at 1630 cm<sup>-1</sup> corresponds to the C=O group; it can be seen also that the intensity of the peaks observed at 1880 and 1900 cm<sup>-1</sup>, the ones due to the formation of nitrous oxide, increase. A summary of these results is given in table 4. Thus, these results show that the inhibitory effect of *C.*

*ambrosioides* extract on the corrosion of 1018 carbon steel in 0.5 M H<sub>2</sub>SO<sub>4</sub> is due to the presence of compounds such as nitrates which are inorganic, passivating inhibitors that have been used satisfactorily in many corrosive environments [27-29].

#### 4. CONCLUSIONS

A study of the inhibitory effect of *Chenopodium ambrosioides* leaves extract on the corrosion of 1018 carbonsteel in 0.5 M H<sub>2</sub>SO<sub>4</sub> has been carried out. Results have shown that *Chenopodium ambrosioides* extract acts as a good corrosion inhibitor, with its inhibition efficiency reaching its highest value at 25 ppm; the inhibitor efficiency decreases with either lower or higher inhibitor concentrations, increases with increasing the temperature and with an increase in the acid concentration. Additionally, the inhibitor efficiency reaches a maximum value after 12 hours of exposure and it decreases for longer exposure times. It was found that the inhibitory effect is due to the presence of nitrates on the extract.

#### References

1. H. Ashassi-Sorkhabi, M. Es'haghi, *J. Solid State Electrochem.* 13(2009):1297.
2. K.F. Khaled, *J. Solid State Electrochem.* 11(2007):1743.
3. M.Z.A. Rafiquee, S. Khan, N.Saxena, M.A.Quraishi, *J. Appl. Electrochem* 39(2009):1409.
4. H. Ashassi-Sorkhabi, E. Asghari, *J. Appl. Electrochem.* 39(2009):631.
5. M.A. Quraishi, A. Singh, V.K. Singh, D.K. Yadav, A.K. Singh, *Mater. Chem. Phys.* 122 (2010):114.
6. A.Y. El-Etre, *Mater. Chem. Phys.* 108(2008):278.
7. A.Bouyanzer, B. Hammouti, L. Majidi, *Mater. Letters* 60(2006):2840.
8. K.O. Orubite, N.C. Okafor, *Mater. Letters* 58(2004):1768.
9. G.O. Avwiri, F.O. Igho, *Mater Letters* 57(2003):3705.
10. I.B. Obot, N.O. Obi-Egbedi, *J. Appl. Electrochem.* 40(2010):1977.
11. K.W. Tan, M.J. Kassimi, *Corros. Sci.* 40(2011):1977.
12. P. Lowmunkhong, D. Ungtharak, P. Sutthivaiyakit, *Corros. Sci.* 52(2010):30.
13. O.K. Abiola, J.O.E. Otaigbe, O.J. Kio, *Corros. Sci.* 51(2009):1879.
14. Khaled KF (2008) *Mater Chem Phys* 112:104
15. F.S. De Souza, A. Spinelli, *Corros. Sci.* 51(2009):642.
16. C.A. Loto, R.T. Loto, A.P.I. Popoola, *Int. J. Electrochem. Sci.* 6(2011):4900.
17. C.A. Loto, A.P.I. Popoola, *Int. J. Electrochem. Sci.* 6(2011):3264.
18. E.E. Ebenso, H.Alemu, S.A. Umoren, I.B. Obot, *Int. J. Electrochem. Sci.* 3(2008):1325.
19. L. Valek, S. Martinez, *Mater. Letters* 61(2007):148.
20. E.E. Oguzie, *Corros. Sci.* 50(2008):2993.
21. F. Bontiss, M. Lagrence, M. Traisnel, *Corrosion* 56(2000):733.
22. P.B. Raja, M.G. Sethuraman, *Mater. Letters* 62(2008):113.
23. M.A. Amin, S.S.A. El-Rehim, E.E.E. El-Sherbini, R.S. Bayoumi, *Electrochim Acta* 52(2007):3588.
24. M.A. Quraishi, A. Singh, V.K. Singh, D.K. Yadav, A.K. Singh, *The Open Corr. J.* 2 (2009):58.
25. J.C. Da Rocha, J.A.C. Gomez, E. D'Elia, *Corros. Sci.* 52(2010):2341.
26. S.A. Umoren, I.B. Obot, N.O. Obi-Egbedi, *J. Mater. Sci.* 44(2009):274.

27. D. Wang, X. Tang, Y. Qiu, F. Gan, G.Z. Chen, *Corros. Sci.* 47(2005):2157.
28. K.H. Na, Su Il Pyun, *Corros. Sci.* 48(2007):2663.
29. H. Wang, R. Akid, *Corros. Sci.* 50(2008):1142.